ELSEVIER

Contents lists available at ScienceDirect

Scripta Materialia

journal homepage: www.elsevier.com/locate/scriptamat



In situ transmission electron microscopy investigation of nucleation of GP zones under natural aging in Al-Zn-Mg alloy



Arya Chatterjee*, Liang Qi, Amit Misra

Department of Materials Science and Engineering, University of Michigan, MI 48109, USA

ARTICLE INFO

Article history: Received 27 May 2021 Revised 26 September 2021 Accepted 29 September 2021 Available online 7 October 2021

Editor: Beyerlein Irene J.

Keywords:
Al-Zn-Mg alloys
Natural aging
GP zones
In situ heating
Transmission electron microscopy

ABSTRACT

This investigation reveals very early-stage (within an hour) precipitation during natural-aging of Al-Zn-Mg alloy can have very complex processes with strong fluctuations in precipitate types and formation mechanisms. *In situ* heating followed by quenching and subsequent natural-aging at room temperature was carried inside transmission electron microscope to study the formation and evolution of early-stage precipitation. Investigation reveals formation of solute clusters at \sim 2 mins and subsequent nucleation of GP-II zone adjacent to clusters at \sim 10 mins during very early-stage natural-aging. Moreover, nucleation of GP-II is found to be related to GP-I but not in one unique mechanism. GP-I precipitates were observed to act as sites for the formation of GP-II either by 'separated' nucleation (i.e. from the interface between GP-I and Al matrix) or via *in situ* nucleation (i.e. from a GP-I precipitate). Occasionally, some GP-II precipitates were observed to dissolve into Al matrix without further transforming to η' precipitates.

Published by Elsevier Ltd on behalf of Acta Materialia Inc.

7XXX series Al alloys developed for aerospace applications have high specific strength in the peak-aged condition. Their widespread implementation in the automotive industry for body and closure applications can achieve vehicle light weighting goals if the challenges of the component forming and fabrication can be surmounted [1–3]. Conventional automotive mechanical forming processes such as stamping and hemming, involve room temperature forming of Al sheet alloys in the as-quenched state when alloys have high ductility and formability, followed by artificial aging during the paint bake operation. Due to fast (often within 30 minutes after quenching) and continuously varying natural aging characteristics of current 7000 series alloys, the formability decreases very rapidly and keeps changing as the aging time increases [4,5], necessitating costly steps such as warm stamping or coupled solutioning-quenching-stamping operations in a narrow time window [6,7]. The decrease in formability is the result of gradual increase in hardness during natural aging (i.e. aging at room temperature) [8]. It happens through the formation of clusters in Al matrix, where these small clusters act as barriers for dislocation movement during plastic deformation and decrease the

Upon quenching, a high level of super saturation exists for solutes in the Al matrix along with the excess concentration of va-

cancies (than equilibrium condition). Further, these solutes were found to agglomerate at the sites with high quenched-in-vacancies without forming any specific ordered structure; these are referred to as solute clusters in Al-Zn-Mg alloys [9]. Hence, the interface between solute clusters and Al lattice is not defined. When these clusters are found in periodic order and result in strong distinguishable contrast compared to the surrounding matrix, these are referred to as Guinier-Preston (GP) zones, named after their discoverer [10,11]. In Al-Zn-Mg alloys, generally two kinds of GP zones can form from the super-saturated solid solution (SSSS): GP-I and GP-II zones. Earlier works have suggested GP-I zones as linked to solute rich clusters (SRCs) [12,14,15], fully coherent with Al matrix having internal ordering of enriched solutes (i.e. Zn and Mg) designated as AuCu(I)-type [12] or Frank-Kasper σ -type structures [16], and can form between room temperature to artificial aging at 150°C [13]. On the other hand, it was suggested that GP-II zones are related to vacancy rich clusters (VRCs) [12,14,15,17], therefore needs high vacancy concentration [17], and generally believed to form when quenched from above 450°C and aged at temperatures higher than 70°C [12]. GP-II zones are mostly suggested to have Zn enriched atomic layers along the {111} planes in the Aluminum lattice [18]. Some of the researches indicated that GP-I zones transformed to metastable η' phase [17,19], while others showed GP-II zones as precursors to metastable η' phase [12,15,20]. Therefore, precipitation sequences during natural aging were reported to be one of these two sequences mentioned below: [17,21]

• SSSS \to GP-I zones \to Metastable η' phase \to Stable η (MgZn₂) phase

^{*} Corresponding author at: Materials Science and Engineering, University of Michigan, 2300 Hayward St, Ann Arbor, MI 48109, USA.

E-mail addresses: archatte@umich.edu, aryachatterjee10@gmail.com (A. Chatterjee).

A. Chatterjee, L. Qi and A. Misra Scripta Materialia 207 (2022) 114319

• SSSS \to VRCs \to GP-II zones \to Metastable η' phase \to Stable η (MgZn₂) phase

Moreover, it is also reported that not only the size and number density but also the type of clusters and consequently the GP zones may change with time during natural aging [9,13]. However, the formations of GP zones from thee clusters are not well understood [22]. Especially, to the best of our knowledge, no reports can be found on the evolution of GP precipitates from the clusters and among themselves at a very early stage of natural aging. Hence, this investigation will emphasize on reporting the formation and evolution of GP zones in Al-Zn-Mg alloy at the very early stage of natural aging with the help of transmission electron microscopy (TEM) studies coupled with *in situ* heating experiments. The new insights gained in the current study can provide a better understanding of early-stage precipitation in Al-Zn-Mg alloy and act as a reference for future study for facilitating the optimal design of Al alloys.

The Al-Zn-Mg alloy selected for this study was a commercially available Al alloy with a composition (in atomic %) of Al-5.7Zn-2.4Mg-1.4Cu-0.19Cr-0.16Fe-0.06Si. The thermal treatment given to the as-received alloy is as following: first, the sample was solution treated at 490°C for 1 h followed by immediate quenching to room temperature (~25°C). Immediately after quenching, the evolution of GP zones was investigated while samples were kept at room temperature for desired amount of time. The heat treatment schedule is schematically presented in Fig. 1a. For in situ TEM study, three thin foils were made from as-received alloy sheet following the standard focused-ion-beam (FIB) techniques [23]. Natural aging phenomena were studied in situ using a Thermo Fisher F30 twin electron microscope with the aid of a DENS MEMS heating holder (2 samples for 7 times) (see Supplementary File S1) and in an aberration-corrected 300KV JEOL 3100R05 (1 sample for 2 times) using Gatan heating holder.

The as-received microstructure shows the presence of η precipitates, Fig. 1b. As-received sample was naturally aged for more than one year, therefore, the presence of stable η precipitates are expected to remain in the microstructures for Al-Zn-Mg alloys [22,24]. Apart from η precipitates, several other (Mg, Zn, Cu)-rich and Fe-rich precipitates which are typically observed in 7000 series Al alloys are also present owing to the presence of Cu and addition of Fe during production of these commercial alloys [25,26]. Compositional analysis by EDS mapping in HAADF-STEM mode showed the presence of precipitates with Zn as the major component followed by Mg and Cu, such as A, B and E precipitates, whereas precipitates **C** and **D** indicated higher Mg content in these particles followed by the amount of Zn and Cu, Fig. 1b. By approximation, Zn-rich precipitates (i.e. A, B and E) showed MgZn₂(Cu) composition, and Mg-rich particles apparently can have Mg₄(Zn, Cu) (for C) or Mg₂Zn(Cu) (for D) stoichiometry. However, the proportions of Mg, Zn and Cu within these complex precipitates were found to be different in earlier works on 7000 series Al alloy having similar solute contents [25,26]. This is because of the difference in aging conditions experienced by the alloys used in previous works and in the present investigation. Upon heating the as-received samples at normalization temperature of 490°C and subsequent holding at that temperature for more than 45 minutes yielded microstructure without the presence of any large or even nanoscale GP zones, as can be seen from the high-resolution transmission electron microscopy (HRTEM) image in Fig. 1c. This suggests that the microstructure was completely solutionized. Immediately after quenching to room temperature (i.e. natural aging time, t = 2 minutes), the samples showed the speck of solute clusters appearing in the Al lattice, Fig. 1d. The brighter contrast observed in HAADF-STEM mode for these clusters as compared to adjacent Al matrix indicates the presence of Zn in these clusters.

Very fast rate of formation for these solute clusters can only be explained in terms of accelerated diffusion due to the presence of excess quenched-in vacancies, since the characteristic diffusion lengths (\sqrt{Dt}) for Zn/Mg solute atoms under equilibrium conditions are just \sim 1 Å for several hours at room temperature [27,28].

Subsequent in situ study of natural aging phenomena shed light on a few interesting observations, regarding the formation and transformation of GP zones, as discussed below. Among the case studies reported here, one indicates the formation of a solute cluster and subsequent nucleation of GP-II zone (Fig. 2). The video of this in situ natural aging process can be observed in Supplementary File S2. The presence of a solute cluster is located within Al lattice with an enlarged view in the right in Fig. 2a. As the natural aging time (NAT) increases, the lattice structure of the surrounding Al-matrix becomes more prominent, Fig. 2b. The fast-Fouriertransformation (FFT) diffractograms obtained from the cluster surrounding lattice regions showed that the incident electron beam is aligned parallel to <110> direction of the Al grain. At t=13m34s, the solute-enriched atomic layers are started to appear along the $(1\overline{11})$ planes adjacent to the cluster, Fig. 2c. With the increase in NAT, migration of more solutes to the GP precipitate (it is GP-II here because it has several solute-enriched atomic layer along the {111}_{A1} planes) resulted in change in phase-contrast of HREM image [13], and makes the solute cluster less visibly distinct within Al matrix, Fig. 2d. However, with more duration of natural-aging, both the cluster and GP-II zone finally dissolved into the Al matrix,

Another incident shows the separated nucleation of GP-II zone from the interface between a GP-I precipitate and Al matrix, Fig. 3. The video of this phenomenon can be witnessed in Supplementary File **S3**. A few spherical coherent precipitates identified as GP-I zones are selected for further investigation, Fig. 3a. A solute-rich atomic layer started originating from the interface between matrix and a GP-I precipitate (at top-right corner of the image in Fig. 3b). Analysis of FFT diffractogram indicates the orientation $(1\overline{1}1)$ planes in the Al lattice and it is found to be the same as that of the newly formed solute-enriched atomic layers (i.e. yellow dotted lines in bright field image of Fig. 3b). With more time under natural-aging condition, more solute-enriched atomic layers are formed and these layers create a platelet like GP-II precipitate having 3 distinct solute-rich ($1\overline{1}1$) plane (Fig. 3c), and finally dissolved into the Al matrix (Fig. 3d). Berg et al. [12] have also reported the formation of GP-II zones having 2 - 5 atomic layer thick solute-rich {111} plane in Al-Zn-Mg alloys. The thickness of GP-II zones are mostly within 2 - 3 nm except for the GP-II precipitate shown in Fig. 2. These thickness distribution of GP-II precipitates are consistent with the thickness range (2-6 nm) of GP-II depicted in previous researches on Al-Zn-Mg alloy [12].

In another case, in situ nucleation of GP-II zone from a GP-I precipitate has been observed, Fig. 4. The video of this this precipitation study can be seen in Supplementary File S4. In Fig. 4a, three GP-I precipitates can be seen immediately after quenching (at t=2min 8 sec). With the increase in NAT, a GP-II precipitate (named as GP-II₁) with solute enriched atomic layers along $(1\overline{11})$ (delineated by yellow dotted lines) started to emerge from a GP-I precipitate, present at the lower-left corner of Fig. 4b. After more time under natural-aging condition, two more regions with solute enriched atomic layers along $(1\overline{11})$ Al, as can be seen from the contrast difference of these zones with the surrounding matrix area (outlined by yellow dotted lines) started to appear from the same GP-I precipitate (Fig. 4c). These platelet characteristic are referred as GP-II₂ and GP-II₃. At this time, the contrast of GP-II₁ is significantly stronger than surrounding Al matrix with the addition of more solutes [13], Fig. 4c. After some time, GP-II2 and GP-II3 are grown in thickness, while the GP-II₁ become solute lean as can be visualized by the reduction in its contrast in Fig. 4d. This phenomenon

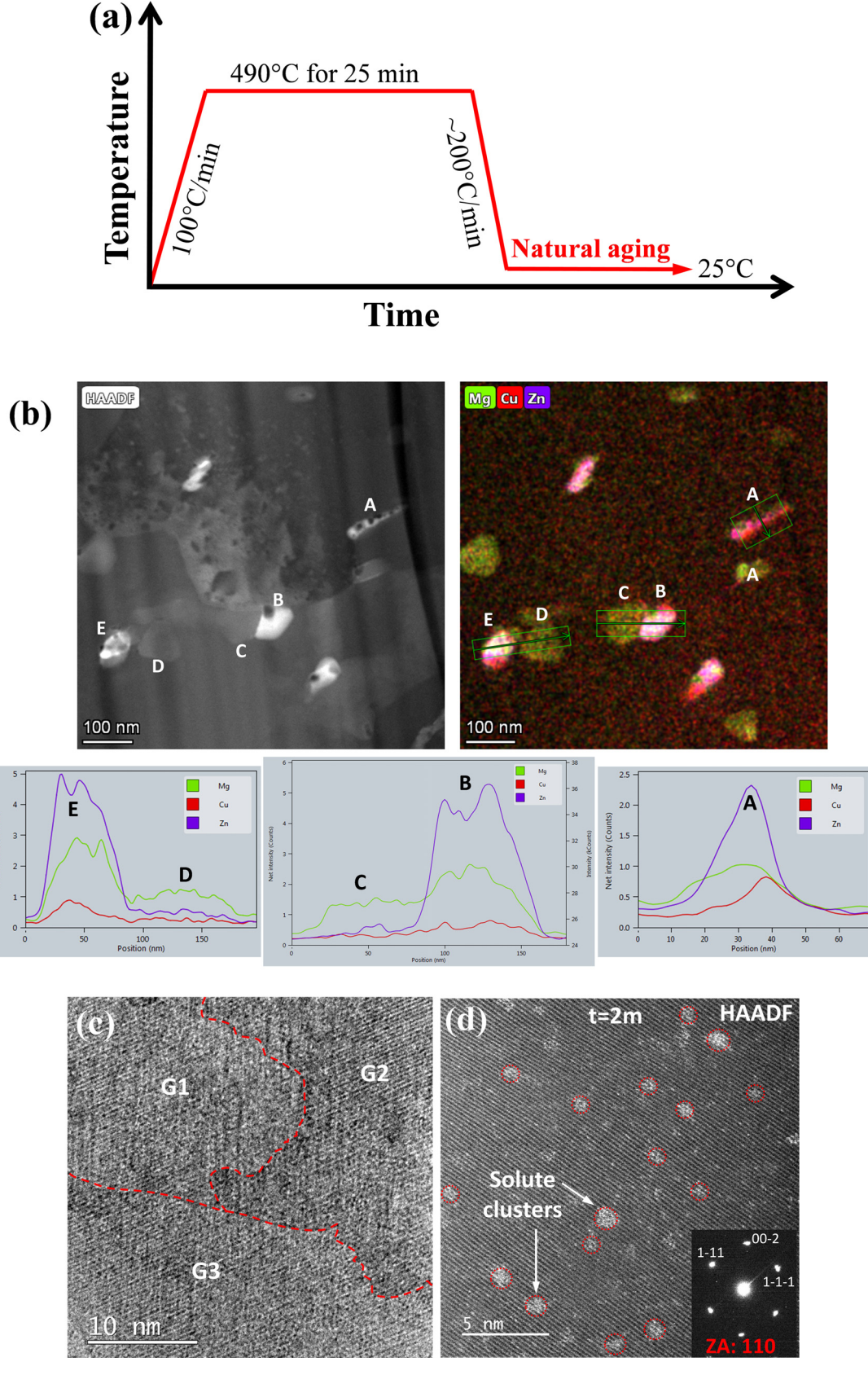


Fig. 1. (a) The schematic representation of the heat treatment schedule used in the current study, (b) As-received microstructure of the material before these were subjected to normalization and subsequent natural aging. The energy-dispersive spectroscopic (EDS) analyses in STEM-HAADF mode exhibit the presence of Zn, Mg and Cu elements in the different kind of stable precipitates present in the microstructure. (c) bright field TEM microstructure of the Al-Zn-Mg alloy sample at 490° C after solutionized for more than 45 minutes. (d) HAADF-STEM image indicating the nucleation of tiny (within 1-2 in diameter) solute-rich clusters in Al matrix immediately after quenching (i.e. at natural aging time, t=2 min.).

A. Chatterjee, L. Qi and A. Misra Scripta Materialia 207 (2022) 114319

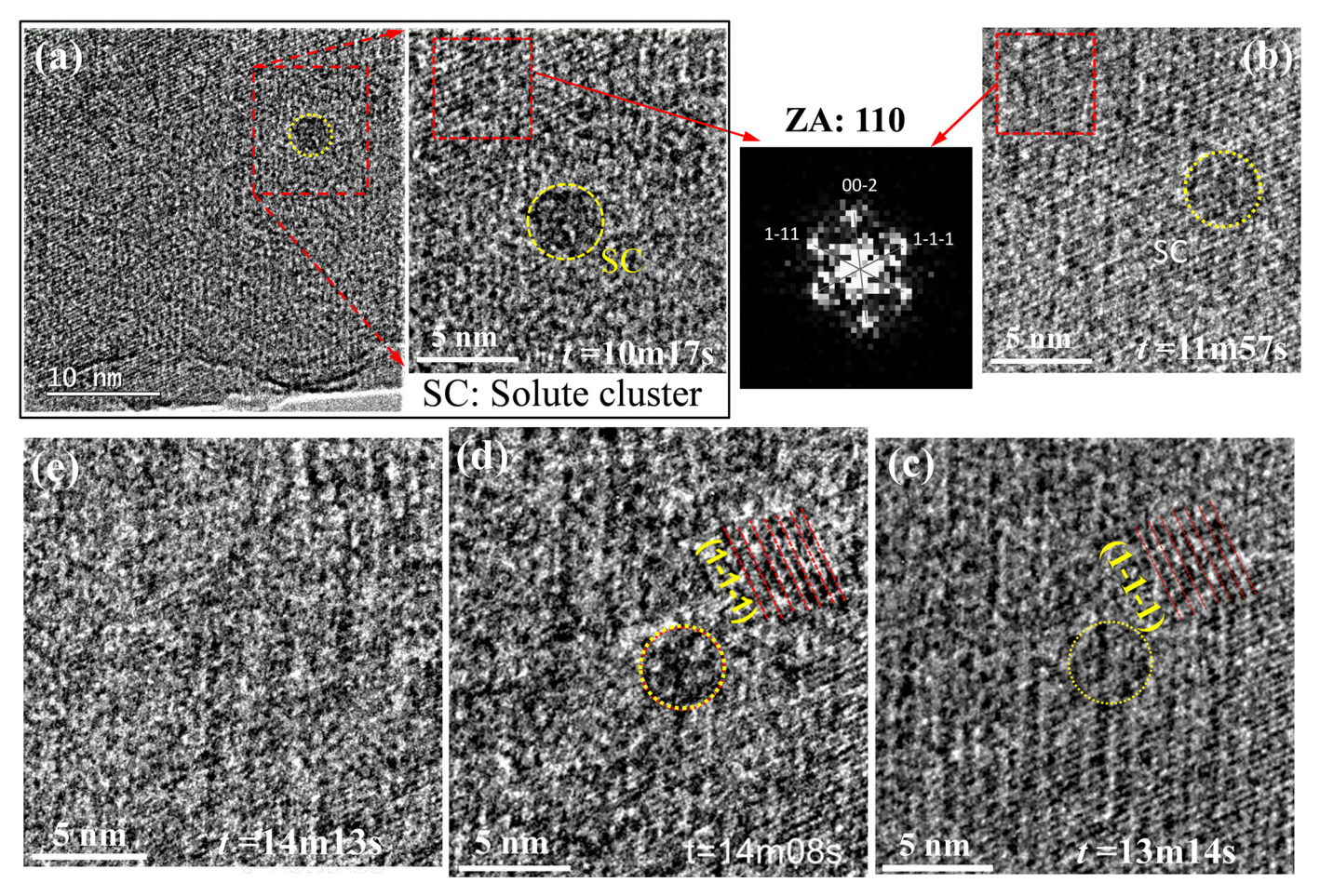


Fig. 2. High resolution transmission electron micrographs obtained at different times during *in situ* observation of natural aging in AL-Zn-Mg alloy. The series of images indicate the formation of solute cluster and subsequent nucleation of GP-II zone adjacent to the cluster. The cluster as well as the GP-II precipitate finally gets dissolved into the Al matrix with the increase in natural aging time. The solute cluster and the GP-II precipitate are delineated by yellow dotted circle and red dotted lines, respectively.

suggests the migration of solutes from the GP-II₁ to both the sides towards GP-II₂ and GP-II₃. With the increase in NAT, the GP-II₁ gets dissolved into the Al matrix, **Fig. 4e**. At this moment, the boundary that defined the chemical ordering of the initial GP-I precipitate as compared to that surrounding Al lattice region [9] becomes less distinguishable suggesting significant solute migration to facilitate the formation and growth of GP-II zones from this GP-I precipitate shown in **Fig. 4e**.

Although direct investigation on the chemical composition of solute clusters or GP zones have not been carried out in the current study, positron annihilation spectroscopy analyses suggested possible clustering of Zn and Mg along with Cu atoms to form solute clusters in Al-Zn-Mg-Cu alloys, where Mg being less active species for clustering [9]. Moreover, co-clustering of Zn and Cu was not ruled out completely. Brighter contrast of the initial solute clusters observed in HAADF-STEM image of the quenched sample (in **Fig. 1d**) suggests the richness of Zn/Cu in these clusters. Xu et al. [18] has also observed presence of Zn in clusters formed during early-stage aging at 150°C. The core of those clusters was Mg-rich. However, the present investigation has not indicated such phenomenon. This can be attributed to the difference in the aging temperature for their work (at 150°C) and the current study (at room temperature, ~ 25 °C), which altered the extent of migration for Mg atoms to join the clusters. Previous works on Cu-containing Al-Zn-Mg alloys showed the presence of Cu in GP precipitates as Mg has a strong tendency to bond with Cu during the initial chemical ordering of GP zones [17]. The smaller Cu atoms might compensate the compressive strain caused by the larger Mg atoms, and

therefore stabilize the Mg-rich spherical solute clusters/GP-I precipitates that might not be stable otherwise. Since the clusters are stabilized, the formation of GP-II zones from solute clusters and GP-I zones can be promoted; similar to as the thermal stability of GP zones enhanced the nucleation of η' precipitates [29]. As the incorporation of Cu is expected to reduce the strain field in GP zones, possibly due to this platelet-shaped GP-II precipitates are found to be grown longer/thicker (see Fig. 2d, Fig. 3c and Fig. 4d) without losing coherency with the Al matrix along the {111}_{Al} habit planes [20]. Addition of Zn-rich atomic layers on $\{111\}_{Al}$ planes reported to have contributed for the growth of GP-II [18]. Although nucleation GP-II from GP-I via in situ nucleation (i.e. from GP-I) and separated nucleation (i.e. from the interface between GP-I and the Al matrix) has not been reported previously, Chung et al. [22] has observed separated nucleation of η' from the region adjacent to GP-II and in situ nucleation of η from η' . The driving force for the observed dissolution of GP-II precipitates in Al lattice with increased natural aging time, without transforming into stable η' precipitates as reported in the previous works [12,15,20], suggest fluctuations in the dynamics of solute cluster evolution.

The present very early-stage precipitation study in Al-Zn-Mg alloy under natural aging condition exhibits the formation of solute cluster and subsequent nucleation of GP-II zone adjacent to the cluster immediately (from within \sim 5 mins to \sim 1 hour) after quenched down to room temperature from the normalization temperature of 490°C. The relation between GP-I and GP-II precipitates in regard to their nucleation during natural aging in the Al-Zn-Mg alloy has been elucidated. The current study indicates

A. Chatterjee, L. Qi and A. Misra Scripta Materialia 207 (2022) 114319

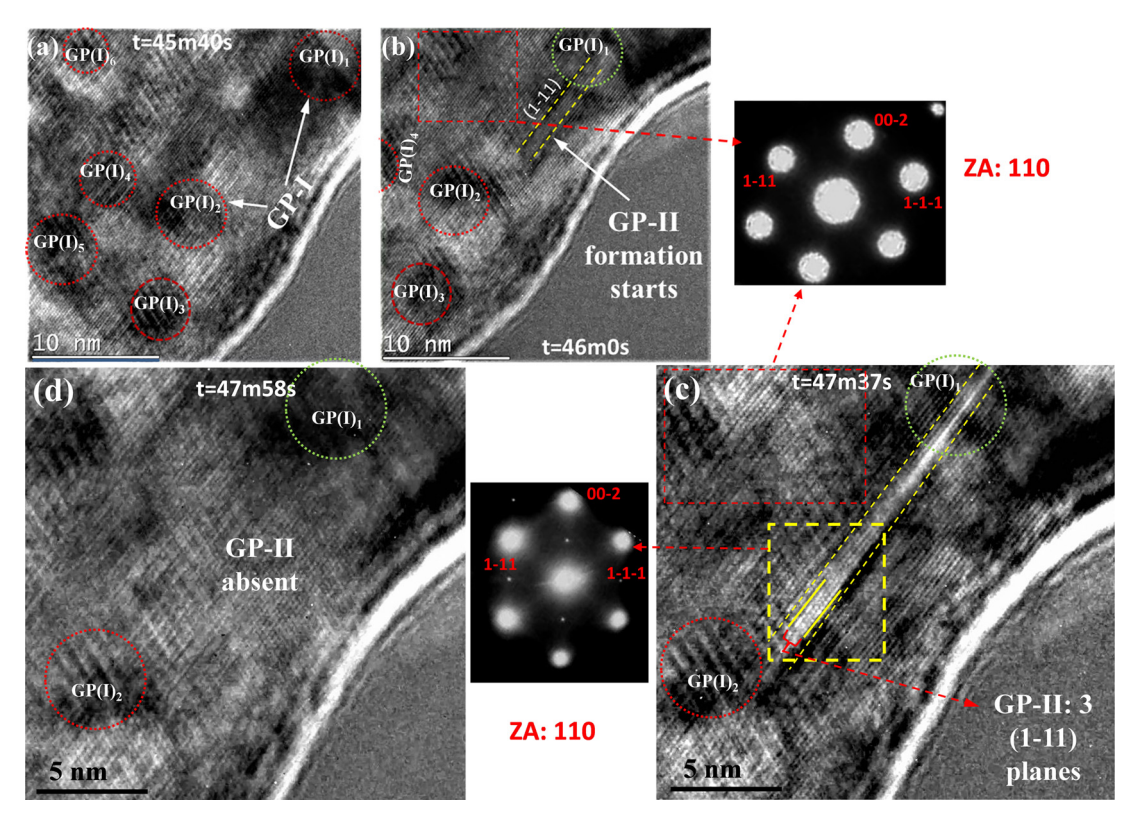


Fig. 3. High resolution transmission electron micrographs obtained at different times during *in situ* observation of natural aging in the investigated Al-Zn-Mg alloy. The series of images indicate separated nucleation of GP-II zone from a GP-I precipitate. The nucleation of GP-II started from the interface between GP-I and Al matrix. This GP-II further grows in thickness and length and finally dissolved into the matrix with the increase in natural aging time. The GP-I precipitates and the GP-II precipitate are delineated by red dotted circle and yellow dotted lines, respectively, whilst the green dotted circle in (b-d) indicated the initial position of the $GP(I)_1$ precipitate. The FFT of red dotted regions in (b) and (c) shows the crystallographic arrangement of Al matrix area, whilst the FFT obtained from yellow dotted region in (c) indicates the characteristic feature of $GP(I)_1$ i.e. streak at $(1\overline{1}_1)$ Al spot.

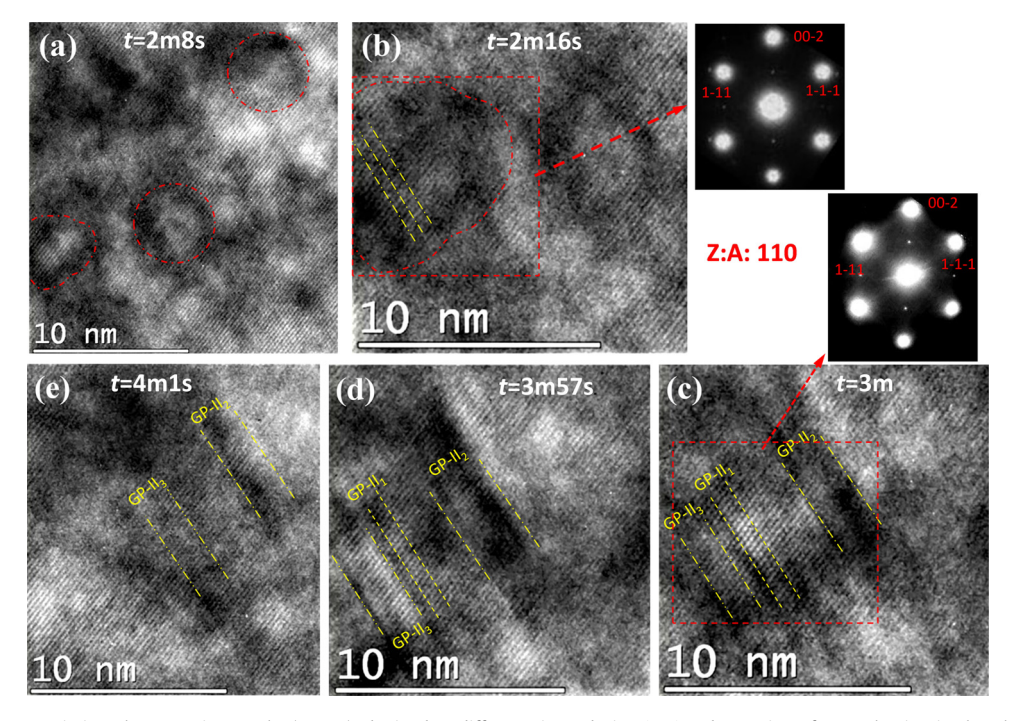


Fig. 4. High resolution transmission electron micrographs (HREM) obtained at different times during *in situ* observation of natural aging in the Al-Zn-Mg alloy. The series micrographs point to the *in situ* nucleation of GP-II zones from a GP-I precipitate (lower-left one in (a)). (b-e): the magnified regions of the image focusing only on that GP-I from which GP-II precipitates are nucleated and subsequently grown or dissolved (GP-II₁) with increase in natural aging time. The GP-I precipitates and the GP-II precipitates are delineated by red dotted circle (in (a) and (b)) and yellow dotted lines (in (b-e)), respectively. FFT from (b) showed weak streak nature at $(1\overline{11})$ Al, whereas, these streaks, which are characteristic feature of GP-II becomes more strong and visible in FFT obtained from (c).

the separated as well as in situ nucleation of GP-II precipitates from GP-I precipitate. Nucleation of GP-II from the interface between GP-I and matrix is referred to as a separated nucleation, whereas when GP-II nucleates from a GP-I is termed as in situ nucleation. Although previous studies suggested GP-II as a precursor to the formation of η' in Al-Zn-Mg alloys, some of these GP-II zones observed in the current study are found to dissolve into the Al matrix without further transforming to η' precipitates. Our results suggest that, although solute clusters and GP zones can start very early (just several mins after the quench from solid solution treatment) during the natural aging, the mechanisms and process to generate stable clusters and precipitates can be quite complex with a relatively long evolution time. Different than the simple precipitation sequences described in the introduction, there could be strong fluctuations in cluster/precipitate types and formation mechanisms. Further investigations are needed to quantitatively understand the critical sizes/time to stabilize these clusters/precipitates. Moreover, the influence of surface effects on the observed phenomena needs to be investigated further.

Declaration of Competing Interest

The authors declare that they have no known competing financial interests or personal relationships that could have appeared to influence the work reported in this paper.

Acknowledgement

This work is financially supported by National Science Foundation (NSF) under Award DMR-1905421. Electron microscopy was performed at the Michigan Center for Materials Characterization, University of Michigan.

Supplementary materials

Supplementary material associated with this article can be found, in the online version, at doi:10.1016/j.scriptamat.2021. 114319.

References

- [1] J. Hirsch, Trans. Nonferrous Met. Soc. China (English Ed. 24 (2014) 1995–2002.
- [2] J. Hirsch, Mater. Trans. 52 (2011) 818–824.
- [3] I.N. Fridlyander, V.G. Sister, O.E. Grushko, V.V. Berstenev, L.M. Sheveleva, L.A. Ivanova, Met. Sci. Heat Treat. 44 (2002) 365-370.
- [4] A. Deschamps, Y. Bréchet, Mater. Sci. Eng. A 251 (1998) 200-207.
- [5] S. Liu, C. Li, S. Han, Y. Deng, X. Zhang, J. Alloys Compd. 625 (2015) 34-43.
- [6] J.D. Bryant, Metall. Mater. Trans. A Phys. Metall. Mater. Sci. 30 (1999) 1999–2006.
- [7] D. Li, A.K. Ghosh, J. Mater. Process. Technol. 145 (2004) 281-293.
- [8] E. Hornbogen, J. Light Met. 1 (2001) 127-132.
- [9] A. Dupasquier, R. Ferragut, M.M. Iglesias, F. Quasso, Phys. Status Solidi Curr. Top. Solid State Phys. 4 (2007) 3526-3529.
- [10] A. Guinier, Nature 142 (1938) 569–570.
 [11] G.D. Preston, Edinburgh London, Dublin Philos. Mag, J. Sci. 26 (1938) 855–871.
- [12] L.K. Berg, J. Gjoønnes, V. Hansen, X.Z. Li, M. Knutson-Wedel, G. Waterloo, D. Schryvers, L.R. Wallenberg, Acta Mater 49 (2001) 3443–3451.
- [13] A.K. Mukhopadhyay, Philos. Mag. Lett. 70 (1994) 135-140.
- [14] V. Hansen, O.B. Karlsen, Y. Langsrud, J. Gjønnes, Mater. Sci. Technol. 20 (2004) 185-193
- [15] H. Loffler, I. Kovacs, J. Lendvai, J. O'F, Mater. Sci. 18 (1983) 2215–2240.
- [16] A. Lervik, E. Thronsen, J. Friis, C.D. Marioara, S. Wenner, A. Bendo, K. Matsuda, R. Holmestad, S.J. Andersen, Acta Mater 205 (2021) 116574.
- [17] G. Sha, A. Cerezo, Acta Mater 52 (2004) 4503-4516.
- [18] X. Xu, J. Zhenga, Z. Lia, R. Luo, B. Chen, Mater. Sci. Eng. A 691 (2017) 60-70.
- [19] A.K. Mukhopadhyay, Q.B. Yang, S.R. Singh, Acta Metall. Mater. 42 (1994) 3083-3091.
- [20] Y.Y. Li, L. Kovarik, P.J. Phillips, Y.F. Hsu, W.H. Wang, M.J. Mills, Philos. Mag. Lett. 92 (2012) 166-178.
- [21] J. Lendvai, Mater. Sci. Forum 217-222 (1996) 43-56.
- [22] T.F. Chung, Y.L. Yang, B.M. Huang, Z. Shi, J. Lin, T. Ohmura, J.R. Yang, Acta Mater 149 (2018) 377-387.
- [23] A. Chatterjee, E. Sprague, J. Mazumder, A. Misra, Mater. Sci. Eng. A 802 (2021) 140659.
- [24] T.F. Chung, Y.L. Yang, M. Shiojiri, C.N. Hsiao, W.C. Li, C.S. Tsao, Z. Shi, J. Lin, J.R. Yang, Acta Mater 174 (2019) 351-368.
- [25] Y. Deng, Z. Yin, F. Cong, Intermetallics 26 (2012) 114–121.
- [26] X. Fan, D. Jiang, Q. Meng, L. Zhong, Mater. Lett. 60 (2006) 1475-1479.
- [27] J. Merikanto, E. Zapadinsky, A. Lauri, H. Vehkamäki, Phys. Rev. Lett. 98 (2007)
- [28] H. Wu, T. Mayeshiba, D. Morgan, Sci. Data 3 (2016) 1-11.
- [29] A. Deschamps, Y. Bréchet, F. Livet, Mater. Sci. Technol. 15 (1999) 993-1000.